Influence of hemicylindrical obstacle scale and length on an impacting blast wave (PROVISOIRE)

R. Gavart[1], S. Trélat[2], M.-O. Sturtzer[1], N. Chaumeix[3]
[1] ISL, Institut franco-allemand de recherches de Saint-Louis, France
[2] IRSN, Institut de Radioprotection et de Sûreté Nucléaire, France
[3] CNRS, Centre National de la Recherche Scientifique, France

1 Introduction

Nowadays, the protection of infrastructures and persons against damages caused by explosions is a very important field of research and development. The ability to predict the effect of a blast wave on a given structure is not straightforward and relies on experimental investigations **[1]** and CFD modelling **[1, 2, 3]**. The experimental studies are usually conducted in small-scale facilities which allow better monitoring by combining different diagnostics methods **[4, 5]** and providing the ability to better control and vary the conditions for blast waves generation and the interaction with various geometrical configurations. So far, numerous studies have focused on blast waves propagation in air and established empirical laws predicting incident overpressures in free field **[6, 7]**. Regarding the interaction with structures, others have studied the evolution of overpressure at the surface of obstacles **[8, 9]**, or the reflection phenomena occurring when a shockwave encounters an obstacle **[10, 11]** have been investigated. The experiments are needed either to validate empirical methods or to be used for CFD validation.

The aim of the present paper is to provide an experimental study on the blast waves characterization initiated by a solid explosive and their interaction with a rigid obstacle (hemicylinder). The coupling between several pressure transducers signals along the path of the blast wave and a high-speed imaging (BOS) allows (i) the measurement of the overpressure at different locations and (ii) the characterization of the blast wave inception, propagation, and reflection on the hemicylinder. The scaling effect has been addressed by performing experiments located at two different facilities: (i) reduced scale at the IRSN facilities and (ii) a larger reduced scale, twice the scale of IRSN facility, at the ISL facilities.

2 Experimental facilities and methodology

The experiments have been performed using two different facilities allowing to vary the scale of the experiments by a factor of 2 for the study of blast interaction with obstacles. The following describes these two facilities.

Correspondence to: raphael-gavart@orange.fr

IRSN facilities (scale A)

In order to carry out reduced-scale experiments, a 2.40 x 1.60 m blast table was designed by IRSN and located at ArianeGroup Vert-le-Petit site to support a 4-section rigid wooden hemicylinder (400 mm diameter and 1.60 m length) and an explosive charge, shown on top of Figure 1. This table, as described in [7], is composed of numerous wooden square modules (40x40x5cm). All these modules are drilled in order to host pressure sensors, one every 133mm. A special module designed to stand the explosion is made of steel to support the explosive charge and detonator. All these pieces make the table highly modular, allowing the flexible positioning of the explosive charge and the pressure sensors on the table. This also allows the adjustment of the hemicylinder to charge distance ranging from 0.27 to 1.60 m. The table was designed so as to minimize vibrations and shockwaves transmission between the modules.

Five pressure sensors are placed along the arc of the hemicylinder with a gap of 30° of angle between each of them, making a sensor at 30°, 60°, 90°, 120°, and 150°. A line of sensors is directly aligned with the charge, with a second line parallel to the first one, shifted by 10cm.

IRSN uses two types of sensors: 603B and 603CA Kistler sensors are piezoelectric sensors, whereas XTL190 Kulite ones are piezoresistive. Kistler (resp. Kulite) sensors are connected to Kistler 5011 (resp. Vishay) charge amplifiers, which are then connected to a 500 kHz Genesis acquisition system (Bridge 1M iso Card) filtered at 125 kHz (FIR filter, -0.1dB cut-off frequency).

ISL facilities (scale 2*A)

ISL designed a blast measurement pad located at its experimental test range. This concrete blast pad represents a scale 2 version of the IRSN blast table (Figure 1 bottom).

A metallic rail was inserted from the charge support plate to the edge of the pad providing twenty-two available sensor positions, each separated by 266 mm, twice the IRSN distance between sensors.

The ISL 4-section steel hemicylinder (800 mm diameter and 3.2 m length) can be installed at distances from the charge ranging from 0.53 to 3.20 m normally to the rail direction (see. Figure 1). A central line of sensors (30°, 60°, 90°, 120°, and 150°) located on the obstacle surface follows the rail axial line with a secondary line of sensors separated by 50mm.

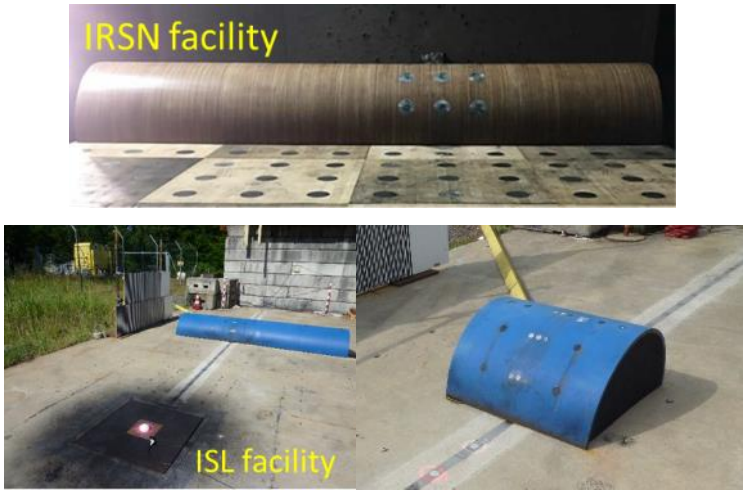

Figure 1: IRSN blast table and ISL blast pad with long/short hemicylinder setup

The main line of sensors is equipped with five PCB 113B28 piezoelectric pressure gauges, while the second one is equipped with five Kulite XT190 piezoresistive pressure sensors. These sensors are inserted in the hemicylinder with a polypropylene insert. Data are recorded and filtered (5^{th} order Bessel filter, 500kHz) by a 2MHz Transcom Recorder.

For each configuration studied at ISL, four series of tests are carried out.

Methodology and experimental conditions

For IRSN experiments, 42g hemispherical Hexomax® (50g TNT equivalent in overpressure) charges are formed manually in a metallic mold and ignited by a Davey-Bickford SA4201A detonator. Therefore, ISL experiments are realised with 333g Hexomax® charges and ignited by a Teledyne Defense RP83 detonator. Examples of explosive charges are shown in Figure 2. Each specific condition is repeated three times at IRSN facility, four times at ISL Facility, in order to ensure the reproducibility of explosive charges and allow for their statistical analysis.

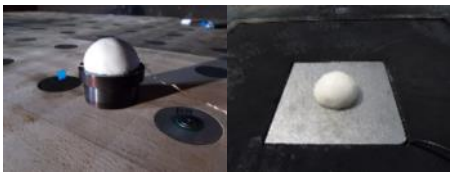

Figure 2: 42g (IRSN facility) and 333g (ISL Facility) Hexomax® charges

Table 1: Characteristics of Tests

Test Configuration	1.6m Long Hemicylinder IRSN	1.6m Short Hemicylinder IRSN	3.2m Long Hemicylinder ISL	3.2m Short Hemicylinder ISL
Number of tests	3	In progress	4	In progress

All ISL tests are also recorded with a V310 and a V311 Phantom cameras, using a 135mm F/2 Nikon lens, at a frame rate of 10 000 images per second. Repeating each experimental configuration four times allows to extend the studied field of view around the hemicylinder with no image resolution loss. The four series of images are then reassembled thanks to a Python algorithm and images of a calibration object (visible on figure 3).

Figure 3: Raw images and reconstruction of the complete field of view

3 Experimental results

Piezoelectric and piezoresistive sensors present different behaviours [12] and pressure profiles on the front face of the hemicylinder, but these differences fade away on the back face, as the shock release takes place (Figure 4). A second pressure peak can be observed at 150° which may be caused by the shock reflection on the floor behind the obstacle.

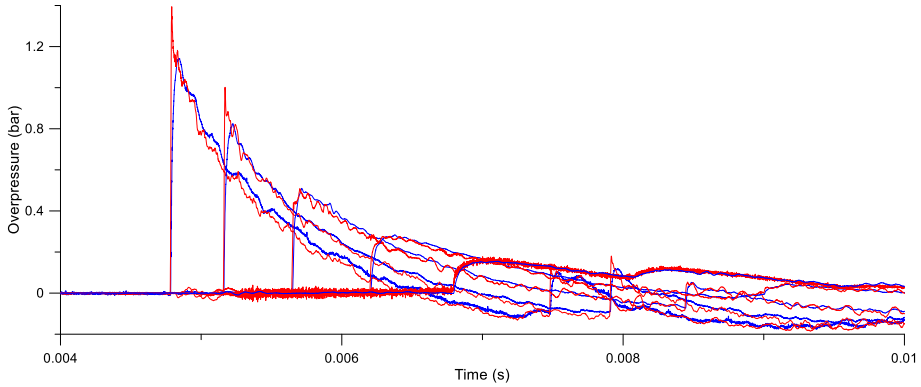

Figure 4: Pressure profiles evolution around a hemicylindrical obstacle (3.2m, 333g Hexomax®) – piezoelectric (red solid line) vs piezoresistive (blue solid line).

Figure 5 represents a comparison between high-speed images recorded for a 333 g Hexomax charge and pressure signals obtained at 120° (white dot representing the sensor position). At this point, the shock wave circumventing the hemicylinder has turned into a Mach stem, which "grows" and curves as the wave goes, and the triple point is propagating above the image superior border.

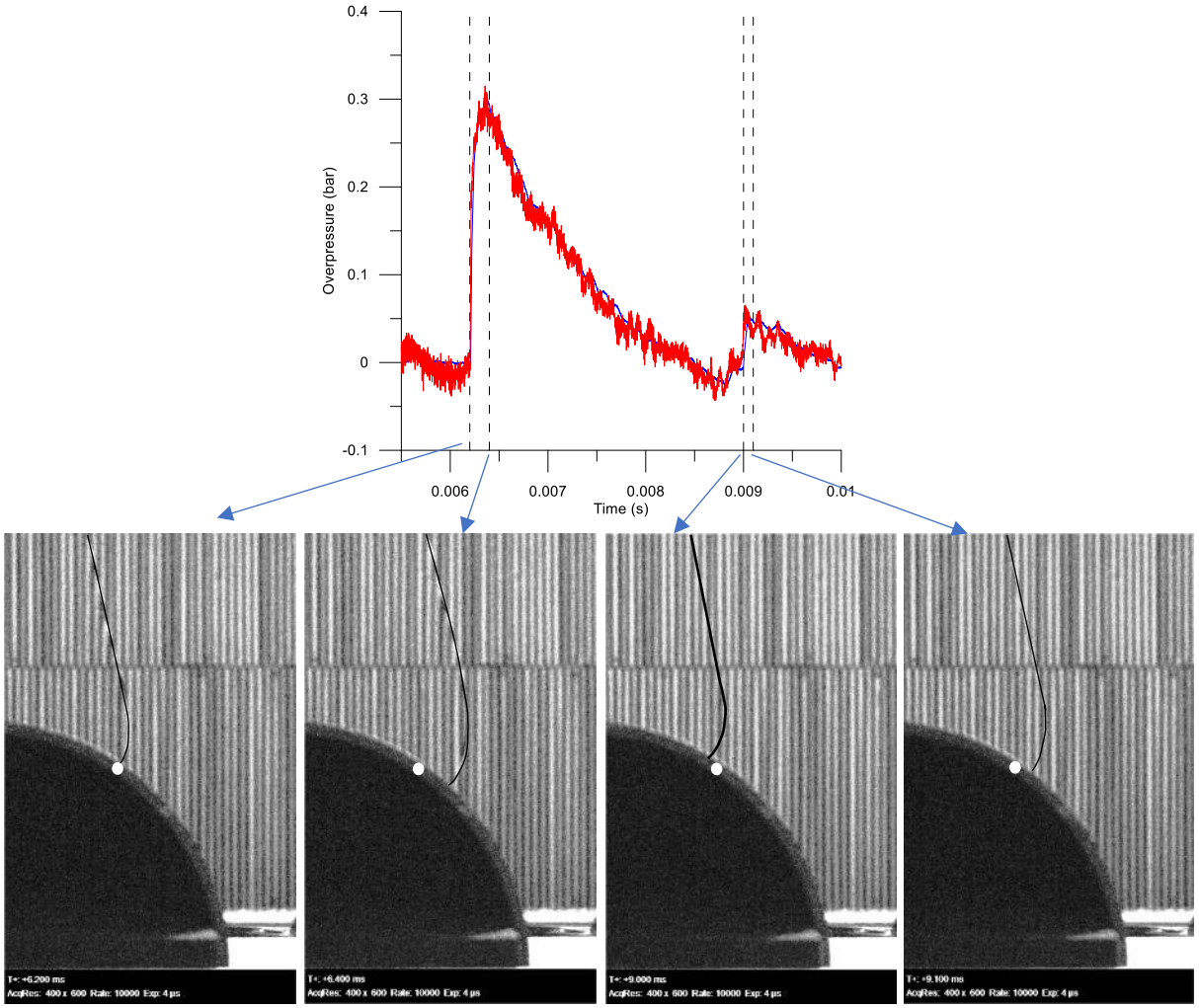

Figure 5: Comparison of a pressure signal with camera images.

Previously, Trélat et al. [5] proposed a phenomenological model for the prediction of the transmission coefficient vs a shifted reduced distance (Figure 6). This model defines the transmission coefficient C_t as the measured overpressure divided by the predicted free-field overpressure at the considered position (eq. 1), and the shifted reduced distance as the direct distance with an origin shifted to the beginning of the expansion zone and divided by the hemicylinder radius (eq. 2).

Eq 1. $C_t = \frac{P_{measured}}{P_{KG}(\lambda)}$ where $P_{KG}(\lambda)$ is the free-field incident overpressure at a distance λ as defined in [6]

Eq 2. $RSDD = \frac{\lambda - \lambda_{lim}}{R}$, where λ, λ_{lim} ($\lambda \geq \lambda_{lim}$) and R are defined in Figure 6

This model has been proposed based on experiments realised at IRSN scale, and it is further described in [5]. Only the overpressure values measured by sensors at 90, 120 and 150° are considered in this study.

In Figure 6, the present results are reported (solid symbols) along with the correlation of the S model (dashed blue line). As we can see, the new dataset obtained for the 42 g Hexomax case (scale 1) falls very well with the S-model for an RSDD of 0.111 (2.5% deviation) and 0.595 (9.7% deviation), which is expected as it is within the conditions for which this model has been validated, but the deviation is larger for an RSDD of 0.934 (14.3% deviation). For the larger scale, the data from the 333g of Hexomax (scale 2), a good agreement is also observed for a RSDD of 0.111 (7.6% deviation), but a larger deviation from the S model is observed for an RSDD of 0.595 (14.5% deviation) and an RSDD of 0.934 (11.4% deviation).

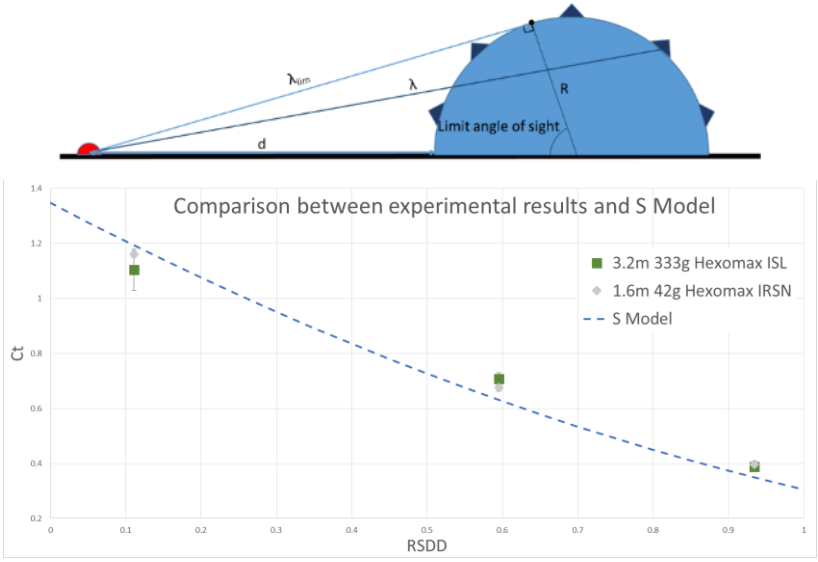

Figure 6: Transmission coefficient evolution depending on reduced shifted direct distance [5]

4 Conclusion

In this paper, new experimental data are reported on experiments performed at 2 different scales using 42g and 333g of Hexomax, as well as several pressure transducers and fast imaging. Overpressure levels generated by blast waves at the surface of a hemicylinder were investigated, which led to convincing results regarding scales' similitude. However, results obtained for larger ISL scale charges are not fully in agreement with a model previously proposed. Tests will need to be carried out at different distances

to verify this tendency. More tests are also planned to investigate the influence of the length of the hemicylinder on overpressure.

References

[1] X.-d. Zhi, S.-b. Qi and F. Fan, "Temporal and spatial pressure distribution characteristics of hemispherical shell structure subjected to external explosion," *Thin-Walled Structures,* vol. 137, pp. 472-486, 2019.

[2] S. Rigby, A. Tyas, T. Bennett, S. Fay, S. Clarke and J. Warren, "A Numerical Investigation of Blast Loading and Clearing on Small Targets," *International Journal of Protective Structures,* vol. 5, no. 3, pp. 253-274, 2014.

[3] C. Tham, "Numerical simulation on the interaction of blast waves with a series of aluminum cylinders at near-field," *International Journal of Impact Engineering,* vol. 36, pp. 122-131, 2009.

[4] H. Kleine, E. Timofeev and K. Takayama, "Laboratory-scale blast wave phenomena – optical diagnostics and applications," *Shock Waves,* vol. 14, p. 343–357, 2005.

[5] S. Trélat, M.-O. Sturtzer and D. Eckenfels, "Multi-Scale experimental study of blast propagation around a hemi-cylindrical barrier," *WIT Transactions on the built environment (ISSN: 1743-3509) - International Journal of Computational Methods and Experimental Measurements - in press,* 2020.

[6] G. F. Kinney and K. J. Graham, Explosive Shocks in Air, Springer Science+Business Media, LLC, 1985.

[7] K. Cheval, O. Loiseau and V. Vala, "Laboratory scale tests for the assessment of solid explosive blast effects. Part I: Free-field test campaign," *Journal of Loss Prevention in the Process Industries,* no. 23, pp. 613-621, 2010.

[8] S. Glasstone and P. J. Dolan, *The Effects of Nuclear Weapons,* United States Departement of Defense & United States Departement of Energy, 1977.

[9] D. K. Ofengeim and D. Drikakis, "Simulation of blast wave propagation over a cylinder," *Shock Waves,* vol. 7, p. 305–317, 1997.

[10] M. Geva, O. Ram and O. Sadot, "The regular reflection/Mach reflection transition in unsteady flow over convex surfaces," *Journal of Fluid Mechanics,* vol. 837, pp. 48-79, 2018.

[11] K. Cheval, O. Loiseau and V. Vala, "Laboratory scale tests for the assessment of solid explosive blast effects. Part II: Reflected blast series of tests," *Journal of Loss Prevention in the Process Industries,* vol. 25, no. 3, pp. 436-442, 2012.

[12] S. Carter, A. Ned, J. Chivers and A. Bemis, *Selecting Piezoresistive vs. Piezoelectric Pressure Transducers,* Application note: AN-102.